JOURNAL OF MATERIALS SCIENCE 22 (1987) 1597–1608

On the testing of diffusion-bonded overlap joints between clad Al–Zn–Mg alloy (7010) sheet

P. G. PARTRIDGE, D. V. DUNFORD
Materials and Structures Department, Royal Aircraft Establishment, Farnborough, Hampshire GU14 6TD, UK

The shear strengths of diffusion-bonded overlap joints between silver-coated clad 7010 Al-alloy sheets of thickness t = 3.2 mm have been determined for various overlap lengths (L) and out-of-plane bending constraints. The measured shear strength decreased with increase in L due to increased bending and peel stresses associated with the asymmetry of the loading path. For overlaps greater than about 1.25 to 1.9 t peel fracture replaced shear fracture as the dominant deformation mode. The bond was more sensitive to peel stresses in the aged state than in the solution heat-treated state. For evaluating diffusion bonds between aluminium-alloys it is recommended that the bond area and L be measured on fracture surfaces and the shear strength be obtained for overlaps in the range L/t = 0.6 to 0.8 using overlap test pieces which are restrained from bending.

1. Introduction

The successful combination of solid state diffusion bonding and superplastic forming in the fabrication of titanium sheet structures [1] has directed attention to the possibility of diffusion bonding aluminium-alloys [2–4]. The reported strengths of diffusion bonds between aluminium-alloys show a wide variation [3–5] depending on the basic bonding parameters (temperature, pressure, time, deformation) and on surface finish, surface coatings, bond interlayers and test piece design. The latter is particularly important since a test piece must provide meaningful strength data to enable the effect of the metallurgical variables on bond strength to be measured.

Single unsupported overlap test pieces are often used to measure the strengths of diffusion bonds [2, 3, 6]. Stress analyses of similar adhesive bonded joints under tensile loads revealed large peel stresses at the ends of the bonded regions [7–12]. These joints failed by bending or under peel stresses and it was difficult to obtain shear failure in the adhesive [10]. Since minor design changes to produce double overlap or strapped joints lead to much lower peel stresses and higher joint efficiencies, the single overlap joint should not be used to carry high tensile loads in adhesive-bonded or diffusion-bonded structures [10, 11, 13]. However, for research or development and for quality control, such joints are easy to fabricate and are of low cost.

Some preliminary tests on diffusion-bonded single overlap joints between aluminium-alloy sheet showed that minimum bending and reproducible shear strengths could be obtained with a jig that held the test piece rigid during testing [14]. Further tests have been carried out to measure the effect of overlap length and out-of-plane stresses on bond strength. The results obtained are described in this paper.

2. Experimental techniques

2.1. Material and ion-plating technique

The sheet had a composition Al–6% Zn–2.3% Mg–1.7% Cu–0.11% Zr (7010) and was heat treated to X166–T7651. The 3.2 mm thick sheet was clad on each surface with Al–1% Zn to a thickness of 4% of the sheet thickness. The areas to be bonded were polished to 1 μm diamond finish, ultrasonically cleaned in acetone and dried in alcohol.

Silver coating was carried out in a Nordiko plant using prior r.f. sputter cleaning followed by d.c. magnetron sputtering of silver. The coating thickness was measured by X-ray fluorescence analysis of a control specimen. The coating and analysis methods are described in detail elsewhere [15]. The silver coatings were $\sim$ 1 μm thick.

2.2. Overlap test pieces

Two types of single overlap test pieces were used. For Type 1 test pieces blanks were 37 mm long × 25 mm wide with two pin holes in each blank. The overlap length, L, was in the range 2 to 9 mm. The test piece is shown in Fig. 1a and a vertical section through a bonded test piece is shown in Fig. 1b. Two sections were cut from the test piece at A and B in Fig. 1a for metallographic examination. For Type 2 test pieces, blanks were 100 mm long × 18 mm wide with a single hole in each blank. The overlap length, L, was in the range 1 to 39 mm. A thicker Type 2 test piece was made by diffusion bonding on to the sheet surface 3 additional sheets. These sheets were not polished prior to silver coating; the test piece is shown in Fig. 2. A double overlap test piece was made using three Type 2 blanks. The centre blank was polished to 1 μm diamond finish on both faces prior to silver coating.

0022–2461/87 $03.00 + .12

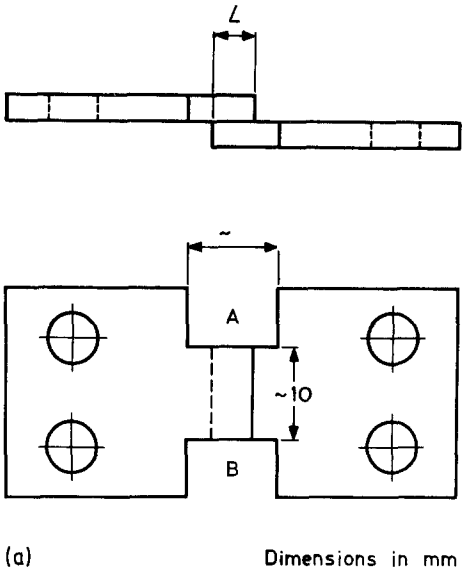

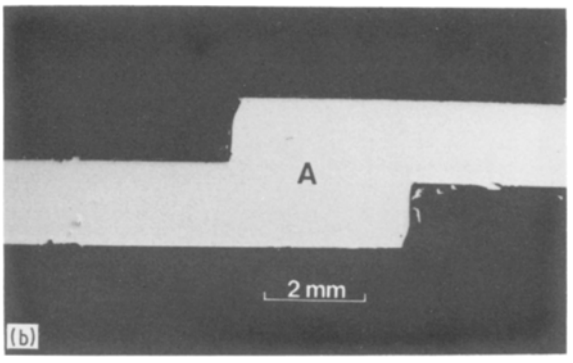

Figure 1 (a) Type 1 single overlap test piece; (b) vertical section through Type 2 bonded test piece.

2.3. Bond interfaces

Three bond interface geometries were investigated as shown in Fig. 3. For Type (a) interfaces, an overlap length, L, on each blank was coated with silver, for Type (b) interfaces, a 5 mm overlap length was left uncoated at the end of each blank, and in Type (c), interfaces a machined step 0.2 to 0.4 mm in height with a length L was machined 5 mm from the end of each blank and the whole blank surface was coated with silver. In the bond area of Type (c) interfaces, only the length L had cladding below the coating.

2.4. Diffusion bonding and heat-treatment conditions

Diffusion bonding was carried out either in argon at 280° C and 120 MPa pressure or in a vacuum of 6×10^{-4} torr at 450° C and 7 MPa pressure for total times at temperatures of $\frac{1}{2}$ and 1 h, respectively. The deformation across the bond was 10 to 14%. The bonded specimens were solution heat treated for 16 h at 480° C and cold-water quenched; the ageing treatment was 24 h at 120° C followed by 10 h at 172° C. The silver layer dissolved in the aluminium during heat treatment [15].

2.5. Testing technique

The single overlap test piece tended to bend under load. Tests were carried out with restraint against out-of-plane bending, and without restraint (Type 2 test pieces only). Three methods were used to modify the local bending. For short Type 1 test pieces a shear test jig was designed to hold the test piece rigid during the test [14]. The jig is shown in Fig. 4; the bond was subjected to a tensile shear stress by a compressive load applied to the outer sleeve. Some Type 2 test pieces were restrained mechanically by loosely clamped plates on the sheet faces as shown schematically in Fig. 5. The loading method for the thick test piece is shown in Fig. 6.

The test pieces were loaded at 0.8 to 2 mm min^{-1} crosshead speed. The net shear stress at failure was calculated by dividing the maximum load by the bonded area determined after fracture. The bonded

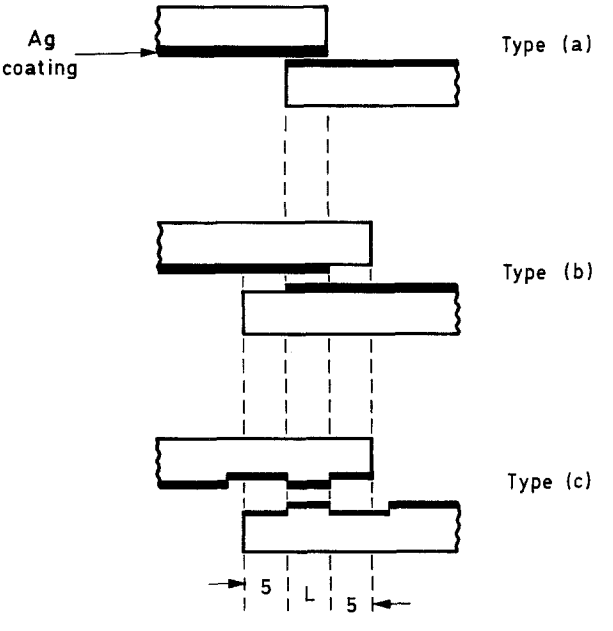

Test piece	Blank dimensions
Type (a)	(1) 37 x 25 wide (2) 100 x 18 wide
Type (b)	(1) and (2) as above
Type (c)	(2)

All dimensions in mm

Figure 3 Diffusion bond interface geometries.

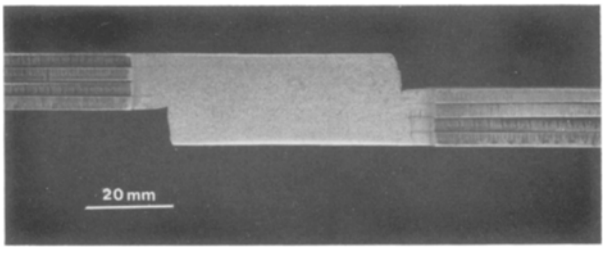

Figure 2 Thick type 2 test piece.

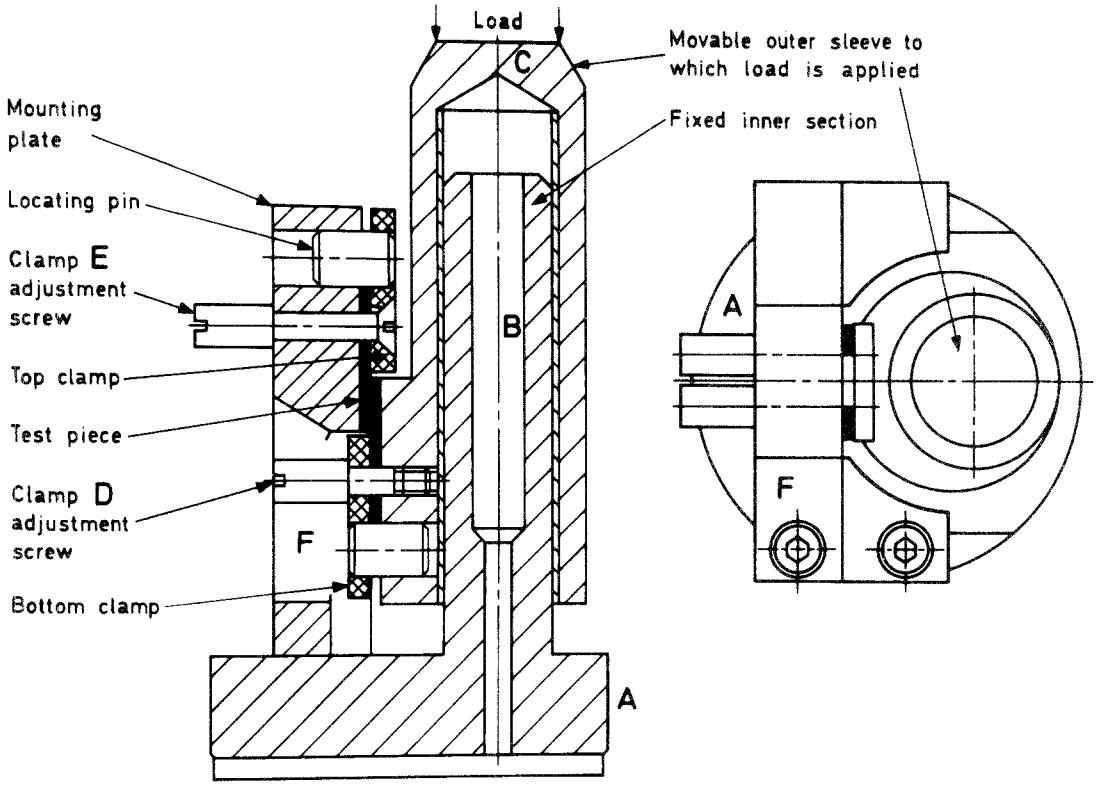

Figure 4 Shear test jig for Type 1 test pieces.

overlap length was measured in sections and on the fracture surface. The tensile properties of the clad 7010 alloy are given in Table I.

3. Results

3.1. Microstructure of diffusion-bonded joints

In the bonded Type 1(a) test pieces the sheet surface above and below the bond remained parallel to the original sheet plane as shown at A in Fig. 1b. However, after etching the bond interface appeared inclined to the sheet plane (at A in Fig. 7a) and the sheet deformation was much greater at the ends of the sheet (at B in Fig. 7a). The inclined interfaces at the ends of the bond are shown at higher magnification in Fig. 8a and schematically in Fig. 8b; after bonding a crack was always present in the bond region B–C and reproducible bonds were only obtained in region A.

With very small overlap lengths (~ 1 mm) the bond interface became inclined about 30° to the sheet plane and was associated with severe local shear in the alloy during bonding (Fig. 9). This deformation caused secondary recrystallization in the alloy (at A in Fig. 9).

In Type (a) interfaces the bond interface inclination increased with increase in bonding temperature. To avoid the increased peel stress component associated with Type (a) interfaces, Type (b) and (c) interfaces (Fig. 3) were introduced. Sections through these interfaces, shown in Figs 7b and c, showed that the interface planes at A remained parallel to the sheet plane and large interface curvatures at the ends of the bonds,

TABLE I Tensile properties of clad 7010 sheet

Conditions	0.2% proof stress (MPa)	Tensile strength (MPa)	Elongation (%)
As-received	486	540	11
SHT (16 h at 480° C)	322	503	15
SHT + age for 24 h at 120° C + 10 h at 172° C	483	536	8

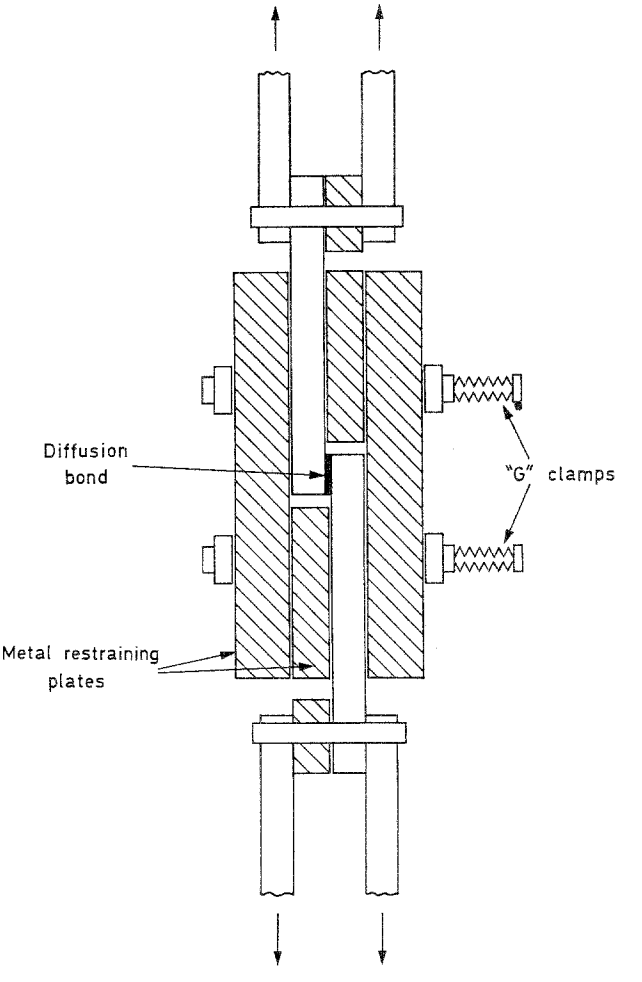

Figure 5 Mechanical restraint for Type 2 test pieces.

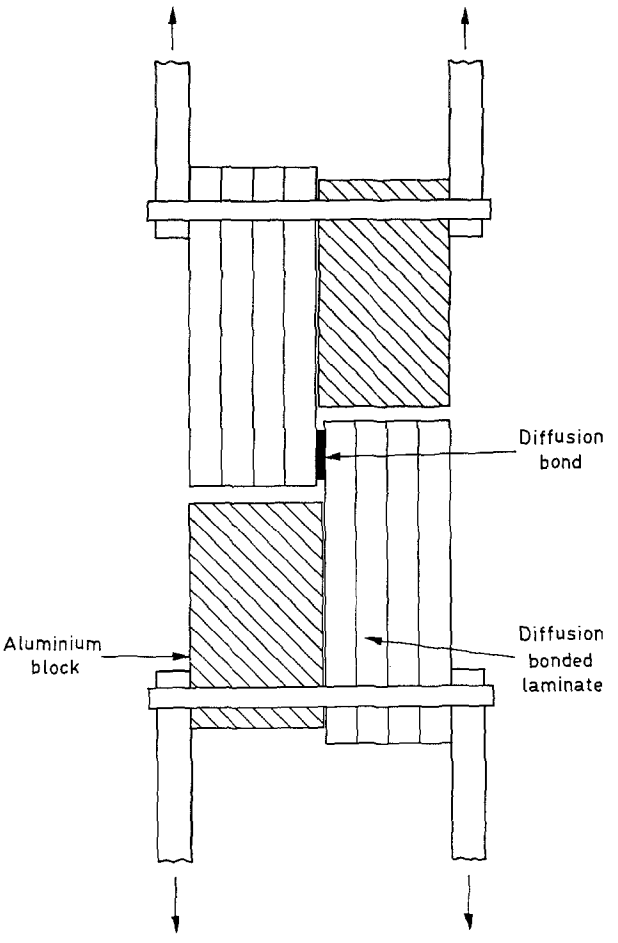

Figure 6 Loading of thick Type 2 test piece.

characteristic of Type (a) interfaces, were avoided. The step at the ends of the Type (c) bond gave rise to a cavity as shown at A in Fig. 10. A disadvantage of Type b and c interfaces was the need to align the blanks carefully during bonding to avoid the mismatch at the ends of the bond as shown at B in Fig. 10.

3.2. Strength of short (Type 1) overlap test pieces restrained in jig

The effect of overlap length, L, on the shear stress and load at fracture is shown in Fig. 11 for material in the solution heat treated (SHT) and SHT and aged state. The stress decreased and the load increased with increasing L. The relationship between the net shear stress and L was approximately linear up to $L \approx 6$ mm with a slope of about 13.5 MPa mm^{-1}. All the test pieces fractured in the bond region. The strengths were the same for Type (a) and (b) interfaces and there was no significant effect of ageing or of bonding temperature. The overlap length, L, is apparent in the fractures at A in Fig. 12a. The restraint imposed by the jig prevented any significant out-of-plane bending of the test pieces (Fig. 12b).

3.3. The strength of long (Type 2) overlap test pieces in the unrestrained state

All these test pieces were bonded at 450° C and 7 MPa pressure. In the SHT state the stress decreased and the load increased with increase in L as shown in Fig. 13. There was no significant difference in the behaviour of (b) and (c) type interfaces. The test pieces with overlaps of about 3, 4, 7 and 9 mm are shown after fracture in Fig. 14. For L = 3 to 4 mm there was little bending of the test pieces, but for $L > 4$ mm significant bending occurred (Fig. 14b). Further evidence of the increased bending with increasing overlap was provided by the load against time curves shown in Fig. 15. For L = 3 mm fracture occurred at maximum load, but for L = 7 to 39 mm there were periods when the load remained almost constant. During these periods the crack grew progressively along the bond region under predominantly peel stresses. The relationship between L and the duration of the peel period is shown in Fig. 16 and indicates that significant peel began above about L = 4 mm. Thus the change in slope of the stress and load curves with increasing L in Fig. 13 corresponds to a change from shear to peel fracture.

Ageing had no effect on the shear stress or load when L = 4 mm but for $L > 4$ mm both load and stress were reduced by ageing and became almost independent of L (Fig. 13). All the aged test pieces fractured at maximum load.

3.4. The strength of long (Type 2) overlap test pieces under restraint

Test pieces in the SHT condition were restrained during testing by longitudinal face plates held by lightly loaded clamps as shown in Fig. 5. The failure

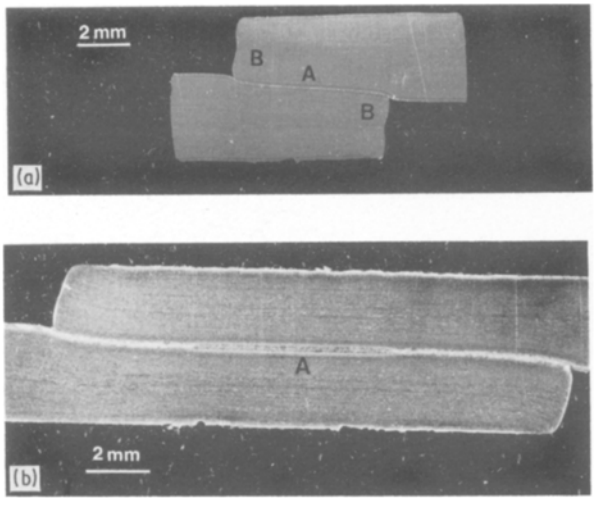

Figure 7 Vertical sections of bond interfaces: (a) type (a), (b) Type (b), (c) Type (c).

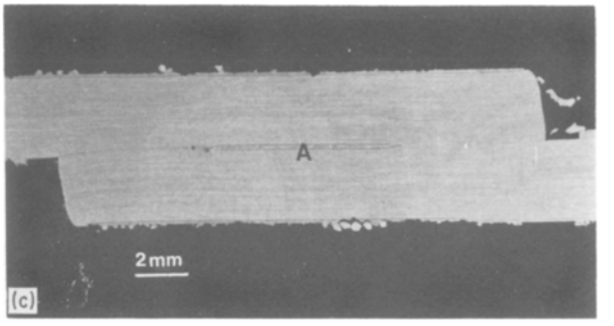

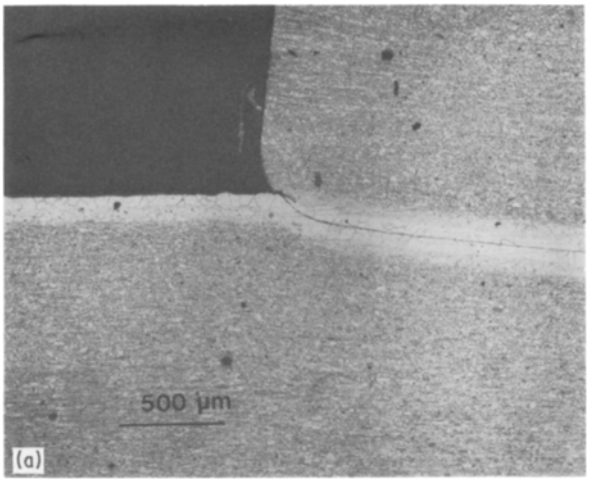

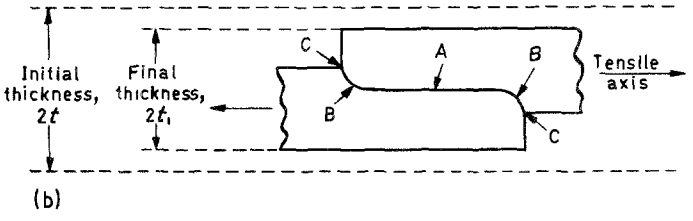

Figure 8 (a) Inclined interface at end of Type 1 diffusion bonds with Type (a) interface. (b) Schematic diagram of Type 1 (a) diffusion bond.

stress and maximum load in this test are compared with the corresponding values for an unrestrained test piece with the same overlap in Fig. 17. Both stress and load were higher for the restrained test piece and in good agreement with the corresponding values for a Type 1 test piece restrained in the jig (Fig. 11). The reduction in bending produced by the restraint is apparent in Fig. 18.

An attempt was made to increase the sheet thickness by bonding on three additional sheets as shown in Fig. 2. The failure load and stress are plotted in Fig. 17 and the fractured test piece is shown in Fig. 19. Failure occurred by delamination of the attached sheets at X which enabled the bond under test to peel at A and B. The residual unbroken bond is shown at C. The stress and load obtained were in good agreement with the values for an unrestrained test piece (Fig. 17).

3.5. Strength of double overlap test pieces

The stress and load against L curves are shown in Fig. 20. For $L \leqslant 6$ mm failure occurred by shear through the bond; for $L \geqslant 18$ mm failure occurred away from the bond by tensile fracture of the central sheet. For $L = 5$ mm the failure load for the double overlap test piece (9.1 kN) was 1.6 times greater than the equivalent unrestrained single overlap (5.7 kN, Fig. 13) and about 1.2 times greater than the equivalent restrained single overlap test piece (8 kN, Fig. 11). Test pieces which fractured in the parent metal are shown in Fig. 21. There was little fracture in the bond in spite of the crack-like notch developed at the ends of the bond at A in Fig. 21, this region was the non-bonded part of the Type (b) interface as shown in the insert to Fig. 20.

3.6. Diffusion bond fractures

The appearance of the fractures depended upon the

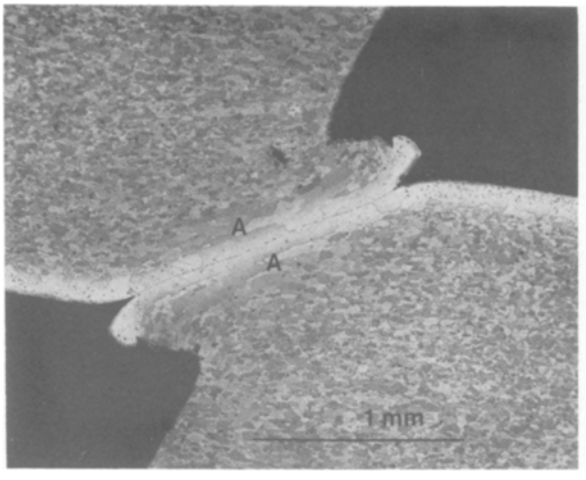

Figure 9 Typical microstructure of small overlap ($L \sim 1$ mm) diffusion bond in Supral 220 aluminium alloy.

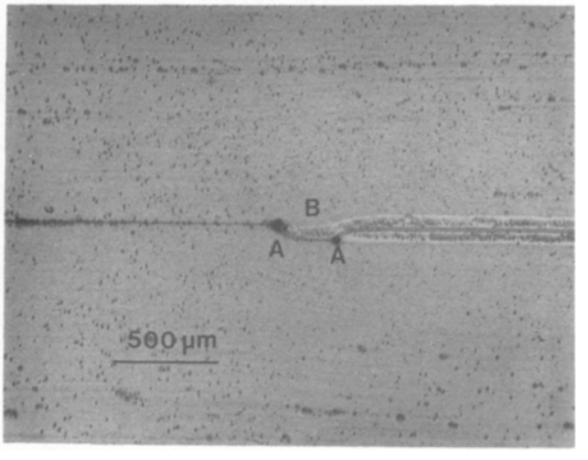

Figure 10 Microstructure of Type 2 single overlap diffusion bond with Type (c) interface.

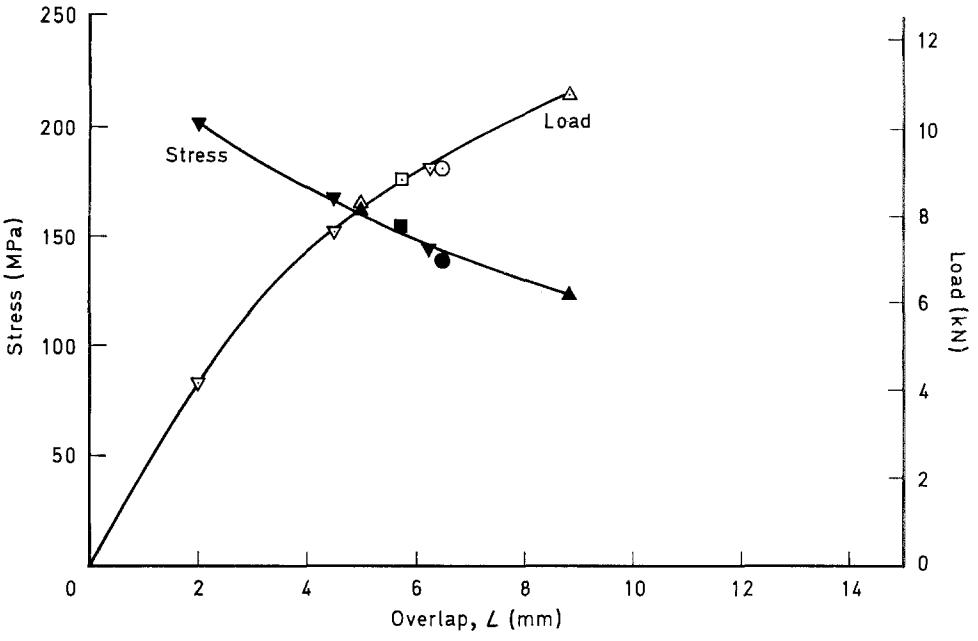

Figure 11 Effect of overlap L on the failure load and stress for Type 1 single overlap diffusion bonds. Bonding conditions: (▲, ▼, ■, ●) stress, (△, ▽, □, ○) load; 280° C, 120 MPa, restrained, SHT (△, ▲) Type 1(a), (▽, ▼) Type 1(b); Aged (□, ■) Type 1(a), 450° C, 7 MPa, restrained, SHT ((○, ●) Type 1(b).

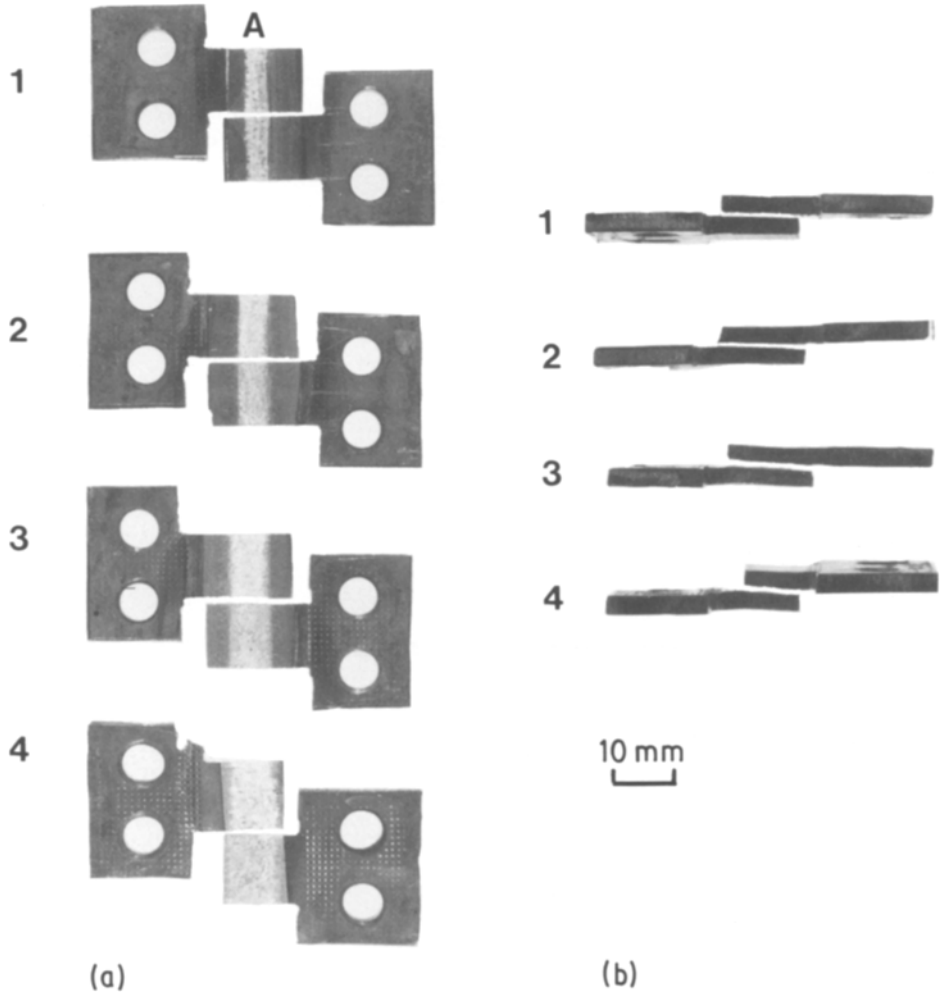

Figure 12 Type 1 single overlap diffusion bonds after fracture. (a) Fracture faces, (b) Edge view of test pieces. (1) L = 2 mm, (2) L = 4.5 mm, (3) L = 6.3 mm, Type (b) interfaces, (4) L = 8.8 mm, Type (a) interface.

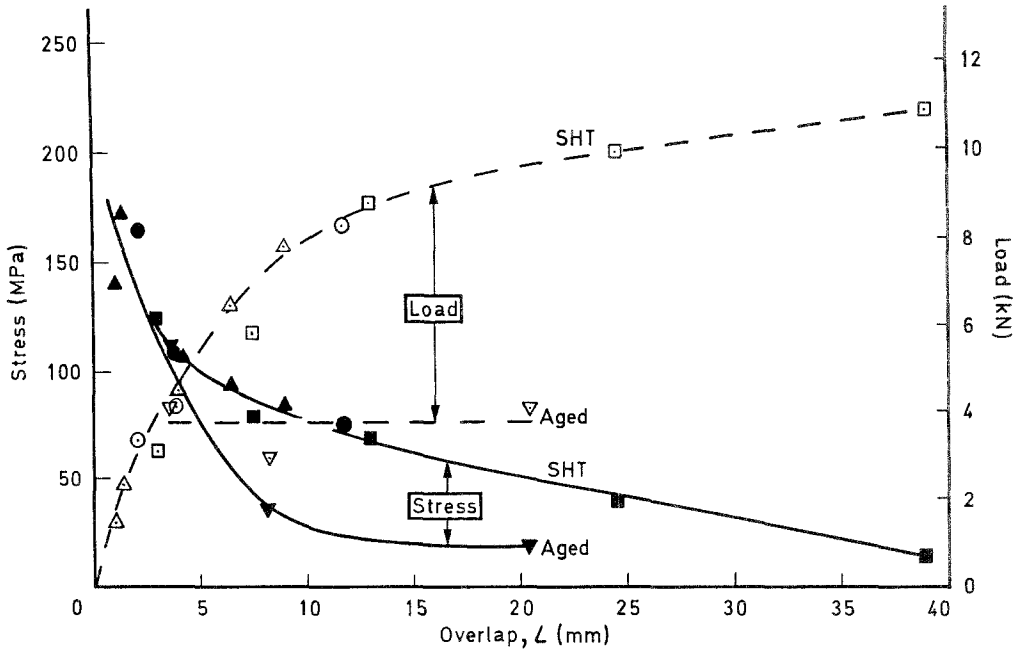

Figure 13 Effect of overlap L on the failure load and stress for Type 2 single overlap diffusion bonds tested in unrestrained state. Bonding conditions: 450° C, 7 MPa, unrestrained. (□, ○, △, ▽) load, (■, ●, ▲, ▼) stress. SHT (□, ■) Type 2(b); (○, ●) Type 2(c), ground ends; (△, ▲) Type 2(c), machined ends; Aged (▽, ▼) Type 2(c), machined ends.

heat treatment. For material in the SHT state there was clear evidence of shear and ductile fracture of the cladding with shear areas at A and ductile fracture cusps on steps at B in Fig. 22. The smooth areas decreased and the area of ductile cusps increased as L increased and peel fracture occurred. Much smoother fractures were obtained after ageing as shown in Fig. 23 and the deformation tended to be confined to a narrow region near the bond interface.

4. Discussion

The results have shown that for solution heat treated material the strengths of single overlap test pieces were very sensitive to the bonded overlap length and to the out-of-plane stresses. Analogous behaviour was found in adhesive bonded metal joints for which the stress distribution is well documented [8, 10, 13]. The apparent reduction in bond shear strength and increase in load to fracture with increasing overlap length are characteristic features of this type of test piece and are caused by the stress concentration at the ends of the bonded sheets and by the asymmetry of the loading path.

4.1. Effect of bending restraint on the measured strength

The shear test jig (Fig. 4) reduced the bending of type 1 test pieces and produced the highest bond shear strengths for $L < 6$ mm (Fig. 11). The maximum shear strength obtained of ~200 MPa is greater than the values reported for sheet roll bonded with 6061 Al-alloy interlayers which produced 147 MPa (2024-T62 Al-alloy) and 142 MPa (7075-T6 Al-alloy) [16] and comparable with the value of 206 MPa reported

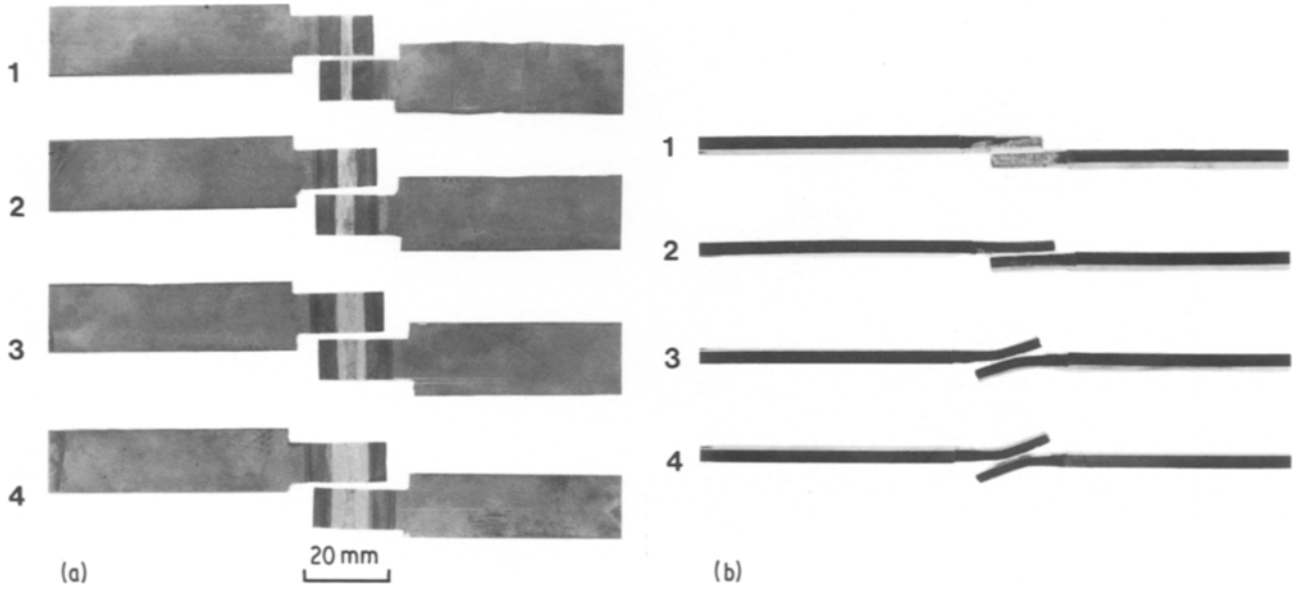

Figure 14 Type 2 single overlap diffusion bonds after fracture in the unrestrained state. (a) Fracture faces, (b) Edge view of test pieces. (1) L = 3 mm, Type (b) interface, (2) L = 4.1 mm, (3) L = 6.8 mm, (4) L = 8.9 mm, Type (c) interfaces.

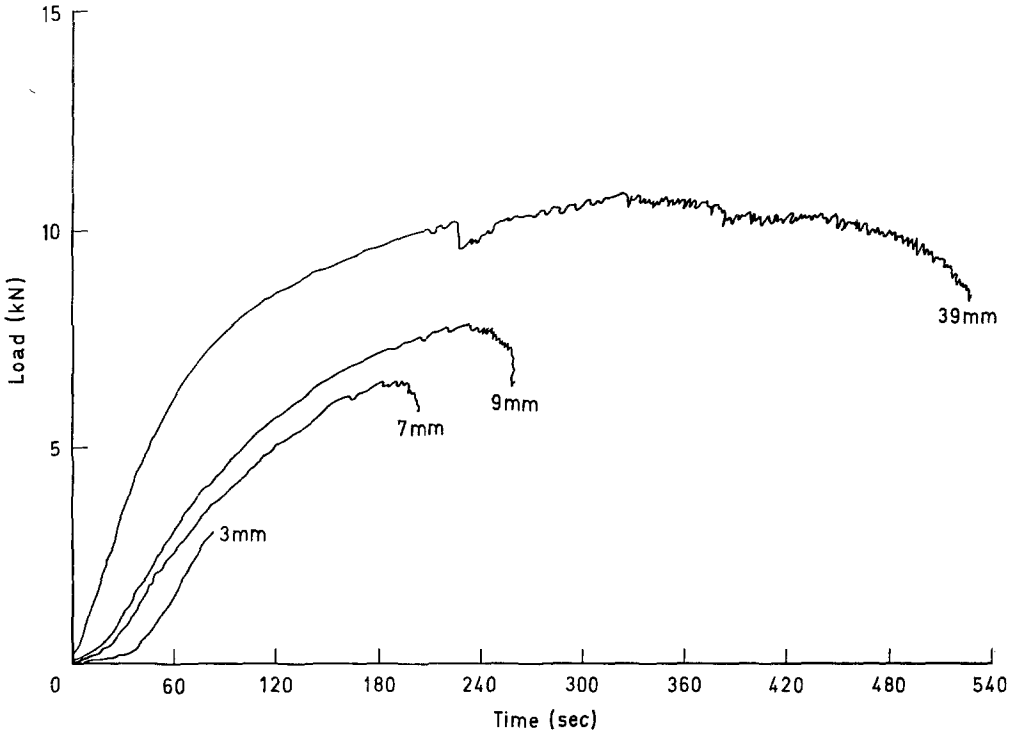

Figure 15 Effect of overlap L on load–time curves for Type 2 single overlap diffusion bonds tested in unrestrained state.

for 7475 sheet bonded with 5052 Al-alloy interlayers [3]. These strengths are 3 to 5 times greater than adhesive-bond shear strengths [2, 16, 17].

A similar high shear strength was obtained by lightly clamping face plates on the test piece during testing (Fig. 17). Without these restraints the test pieces fractured primarily under peel rather than shear stresses. Since the onset of peel prevents high shear stresses being attained, the true shear strength of diffusion bonds cannot be measured with unrestrained overlap test pieces.

The failure loads for restrained and unrestrained test pieces are compared in Fig. 24. Diffusion bonds in the present work were made between clad sheet and the bond shear strength was limited to the shear strength of the clad layer (the silver layer was removed during SHT [15, 17]). The loads measured were greater than the values predicted for failure in the Al–1% Zn clad layer (Fig. 24). This is consistent with the increase in hardness of the clad layer due to diffusion of alloying elements into the cladding [15, 17].

The constant failure load obtained with increase in L for the aged material (Fig. 13) suggests that in this state the bond is sensitive to peel stresses. A reduction in the peel strength was found after ageing [2] and satisfactory peel data could not be obtained for roll-bonded joints in the T6-temper [16].

4.2. Single overlap test pieces

A machined overlap test piece has been used to evaluate adhesive [7] and diffusion bonds [3, 16]. In the latter the test piece was produced by machining a flat-bottomed groove on opposite faces to a depth, t, in the overlap region, with a distance, L, between the

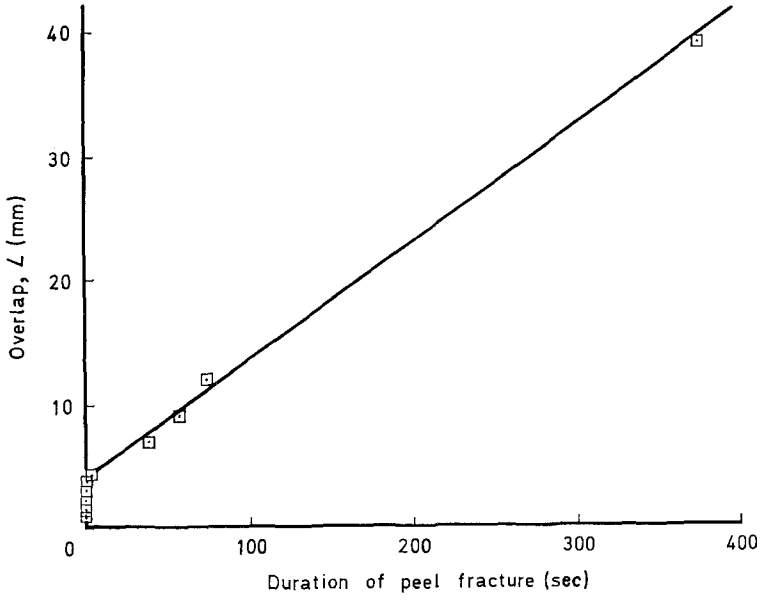

Figure 16 Relationship between overlap L and the duration of peel during testing of unrestrained Type 2 diffusion bonds. Bonding conditions: 450° C, 7 MPa, SHT, Types 2(b) and (c), unrestrained.

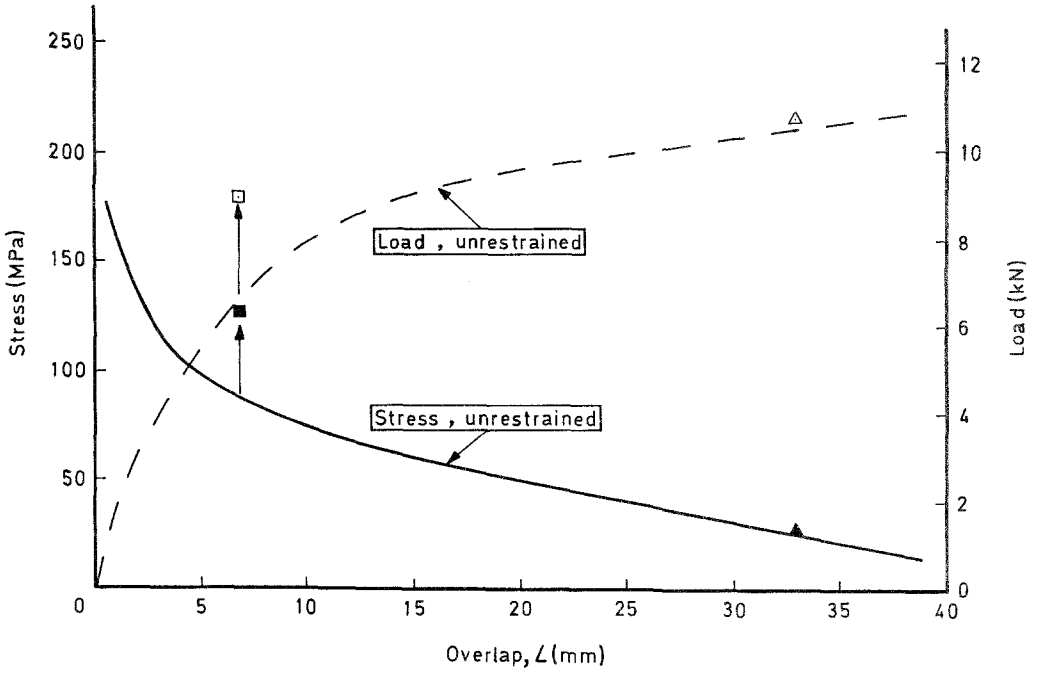

Figure 17 Effect of overlap L on the failure load and stress for Type 2 single overlap diffusion bonds tested in restrained state. Bonding conditions: 450° C, 7 MPa, Type 2, SHT. (□, △) Load, (■, ▲) stress. (□, ■) clamped plates, (△, ▲) thick test piece.

grooves. This test piece has the advantages that it can be produced from bonded panels with accurate overlap lengths, the non-planer bond regions are removed and the test piece is reproducible. Its disadvantages are that it involves a machining operation, the grooves must coincide with the bond line and large bending moments [7] cause bending of unrestrained test pieces [3].

In the double overlap test piece the bending moments are smaller but not eliminated [7], two bonds are tested simultaneously and the test piece is expensive to produce.

It would be difficult to machine grooves in metal matrix composites [13] and simple overlap or more complex joints are preferred for these materials [6, 13]. A single overlap test piece has been recommended for brazed joints [18, 19] and was used to evaluate soldered joints [20]. The Type I test piece, like all single overlap test pieces, has low material and fabrication costs and when tested in the shear jig, it provided reliable quantitative data [14], but special precautions are needed to avoid non-planar bonds and cracks at the ends of the bonded region, although these features did not affect bond strengths in the present tests. It is therefore concluded that the machined overlap test piece or the Type 1 test piece are suitable for measuring bond strengths provided the test procedure recommended in Section 4.3 is followed.

4.3. Comparative strength data

Adhesive and brazed metal bonded joint strengths have been compared with the tensile strength of the adherend using the joint efficiency term (JE) [6, 10, 11] where $JE = P \times 100/\sigma A$, P is the maximum load at fracture for the joint, and σ and A are the tensile strength and cross-sectional area of the adherend, respectively.

For single overlap test pieces, JE values of 43% were obtained for brazed joints between 1 mm thick Al–B composites (L = 12.7 mm, L/t = 12.7) [6]. For similar joints in adhesive bonded 1.28 mm thick 7075-T6 sheet, JE values varied from 32% (L = 3.9 mm, L/t = 5) to 68% (L = 38 mm. L/t = 30) [10]. Since in the present tests σA was a constant JE

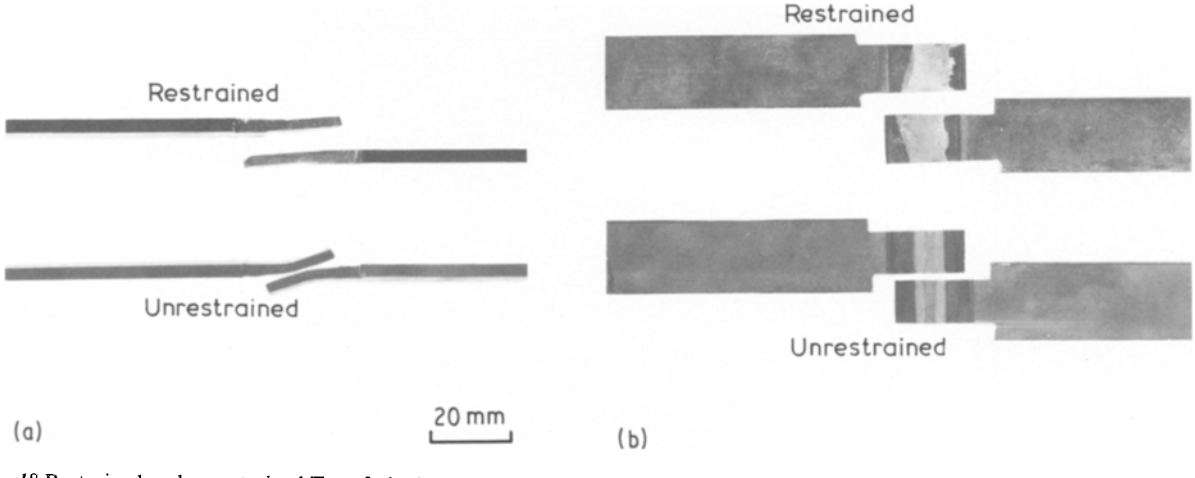

Figure 18 Restrained and unrestrained Type 2 single overlap diffusion bonds after fracture. (a) Edge view of test pieces, (b) Fracture faces.

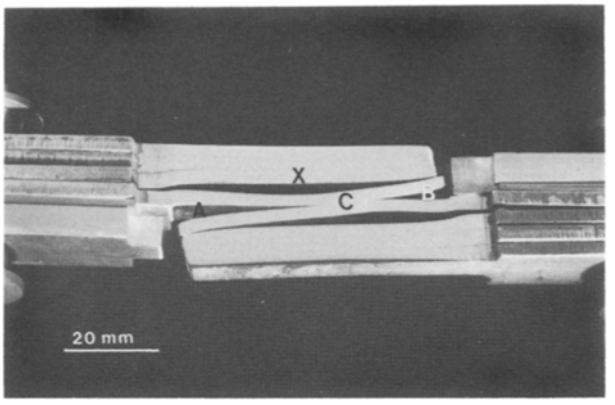

Figure 19 Edge view of thick Type 2 single overlap diffusion-bonded test piece after fracture.

was proportional to P and increased with increase in overlap (Fig. 24). At the maximum overlap used for the Type 1 joint (L = 9 mm, L/t = 2.8) the load was still increasing at P = 11 kN (Fig. 11); since σ = 503 MPa (Table I) and $A = 10 \times 3.2 \times 10^{-6}\,m^2$ the joint efficiency reached 68%. For unrestrained test pieces (Fig. 13) this joint efficiency was not reached until L = 38 mm ($L/t \sim 12$). A joint efficiency of 100%, i.e. parent metal failure was obtained for double overlap test pieces (Fig. 20) with $L > 18$ mm (L/t = 5.6). Clearly JE can be used to compare joint strengths but is not a satisfactory parameter for comparing bond quality or bond shear strength since it does not require bond fracture and when bond fracture does occur, JE increases with increasing peel stress.

A more meaningful measure of these bond properties is obtained by measuring the bond shear ratio $R_B = \tau_B/\tau_p = (P_B/P_p)$ where τ_B and τ_p are the shear strengths of the bond and parent metal, respectively, and P_B and P_p are the corresponding failure loads under shear conditions. In Fig. 24 for $L < 5$ mm fracture occurred in the restrained bonds primarily in shear and the curves indicate the P_B values; these can be compared with the predicted failure loads for the parent metal in shear (P_p). Unlike JE values, R_B values decreased with increasing L, e.g. in Fig. 11 for L = 2 mm, $JE \approx 24\%$ and R_B = 67% and for L = 4 mm, JE = 44% and $R_B \approx 57\%$.

Although the R_B ratio has the advantage that it is directly related to the shear strength of the bond, comparisons must be made with identical test pieces pulled under minimum bending conditions as in the Type 1 tests. Using this test piece, an approximately linear relationship was obtained between τ_p and L in the overlap range 2 to 6 mm (Fig. 11); the slope of the curve was 13.5 MPa mm^{-1} overlap bonded. For τ_B = 160 MPa an error of 1 mm in overlap would give rise to ~8% difference in τ_B and ~4% difference in R_B. In practice it is difficult to control the overlap to within 1 mm [2, 16] and this contributes to the large scatter reported in shear strength data.

To reduce this scatter and to enable the factors affecting the bond shear strength to be quantified the following procedure is recommended. Firstly an accurate measure of the bonded area and overlap length should be obtained from the fracture surface; this will provide accurate stress and L values. Secondly τ against L curves should be determined for each bond variable using $L/t \approx 0.6$, 1.2 and 1.8 where t is the thickness. These data will enable reliable R_B values to be obtained for a given L in this range. This procedure could also be applied to brazed joints for which the multiplicity of joint designs has led to confusing data [18, 19]. Although to optimize joint geometries the designer may still make use of JE values, with increasing process control and reproducibility the trend will be towards a fracture mechanics approach to measuring the strength of diffusion-bonded joints.

5. Conclusions

1. The measured strength of diffusion-bonded overlap joints between silver-coated clad 7010 alloy sheet with thickness t = 3.2 mm, decreased with increase in

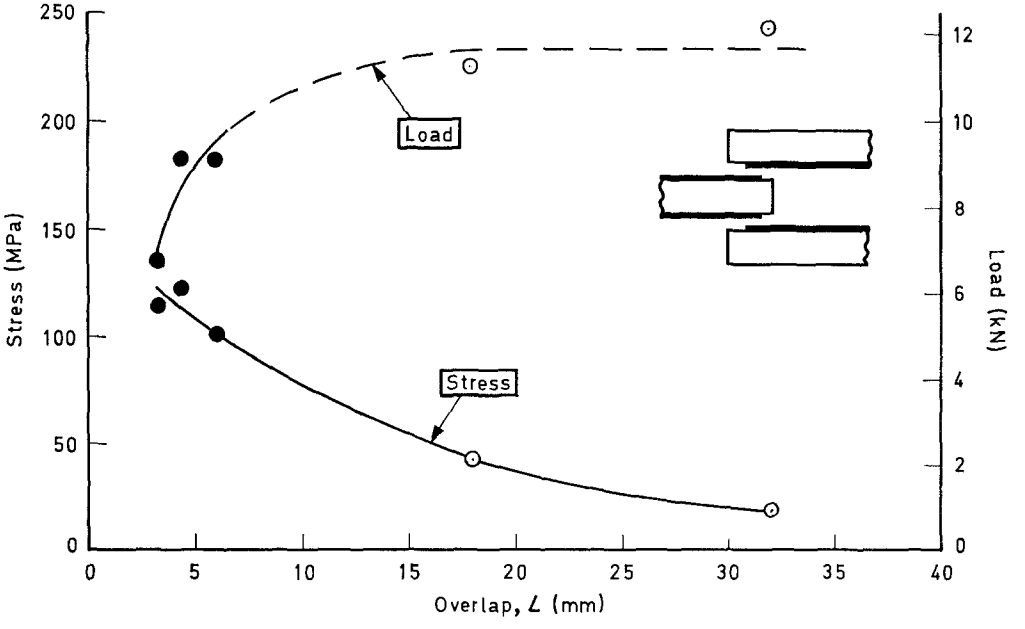

Figure 20 Effect of overlap L on the failure load and stress for Type 2 double overlap diffusion-bonded test pieces. (●) Shear fracture, (○) parent metal tensile fracture. Bonding conditions: 450° C, 7 MPa, SHT, Type 2(b).

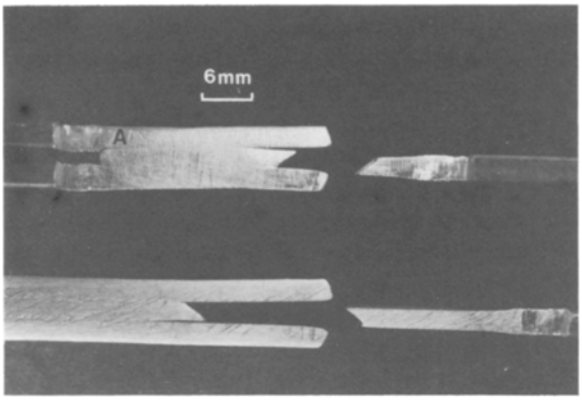

Figure 21 Parent metal fractures in double overlap Type 2 diffusion-bonded test pieces.

overlap length (L) and the strength was lower for unrestrained test pieces.

2. The failure load increased with increase in L for solution heated material but was independent of L for aged material. The different behaviour was attributed to the greater peel stress sensitivity of the aged diffusion bond.

3. For unrestrained test pieces with overlap greater than about 4 mm (L/t = 1.25) peel fracture replaced shear fracture as the dominant deformation mode. This transition in fracture mode occurred at ~6 mm overlap (L/t = 1.9) for constrained test pieces.

4. Errors in overlap length and area measurement or excessive bending and high peel stresses lead to inaccurate bond shear strengths and greater scatter.

5. The following procedure for obtaining reliable shear strengths for diffusion bonds between aluminium-alloys is recommended: (a) a shear test jig should be used to minimize bending of Type 1 or machined overlap test pieces; (b) the bonded area and overlap length, L, should be measured on fracture surfaces to obtain accurate L and stress values; (c) tests should be carried out with L/t in the range 0.6 to 1.8 to enable τ_B–L curves to be plotted; and (d) the bond strength should be compared in terms of the shear strength ratio $R_B = \tau_B/\tau_p$, where τ_B and τ_p are the shear strengths of the bond and parent metal, respectively.

Acknowledgement

This paper is published by permission of the Controller HMSO, holder of Crown Copyright © 1986.

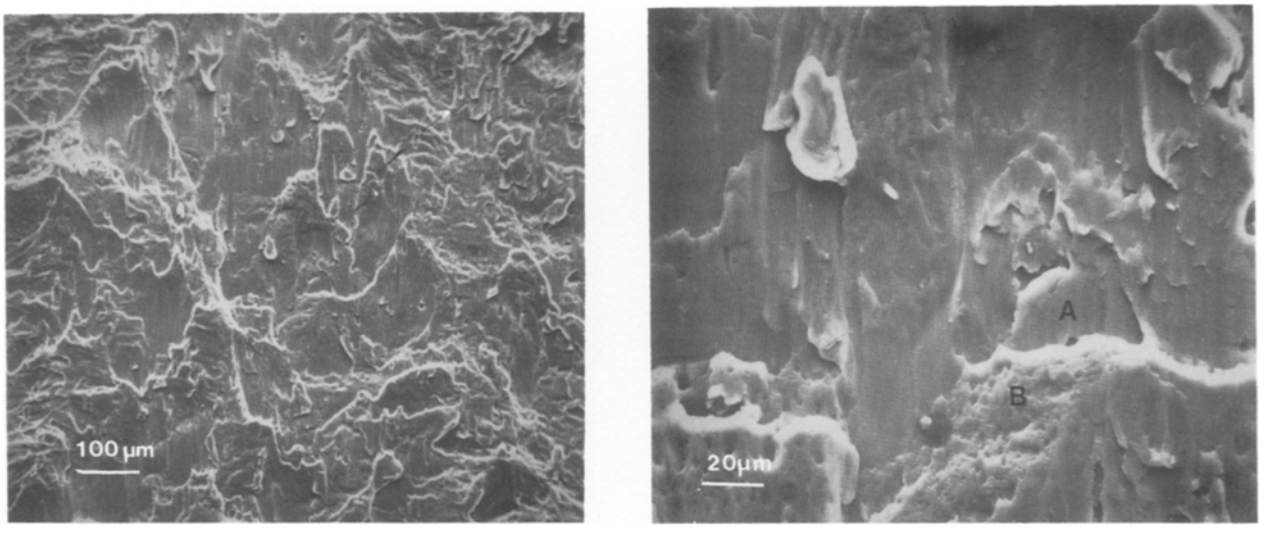

Figure 22 Scanning electron micrographs of fracture surfaces of diffusion bonds tested in the SHT condition.

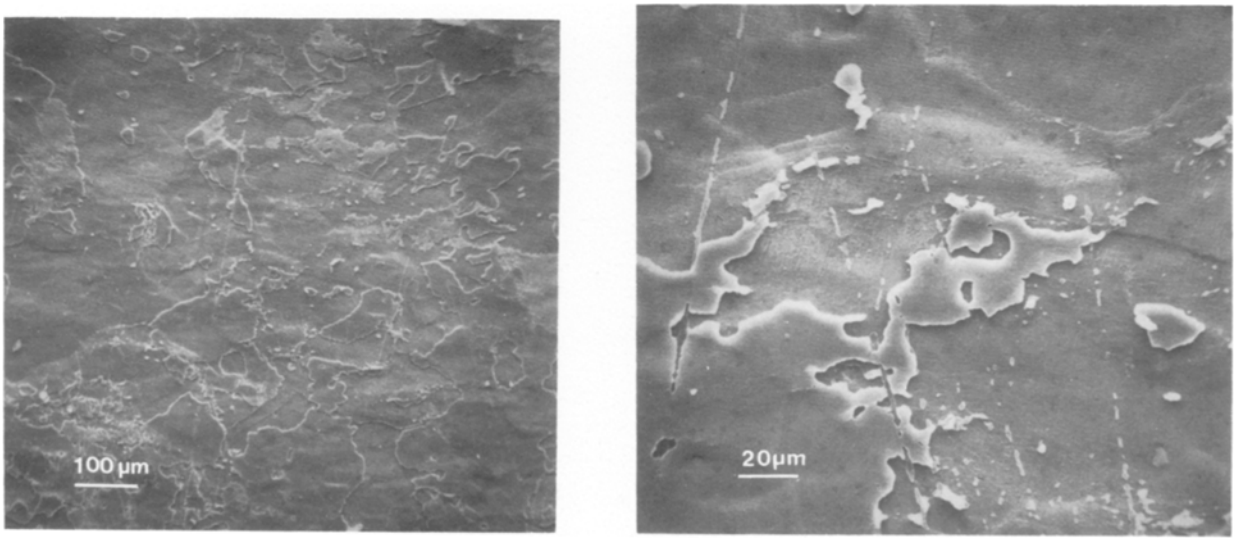

Figure 23 Scanning electron micrographs of fracture surfaces of diffusion bonds tested in the SHT and aged condition.

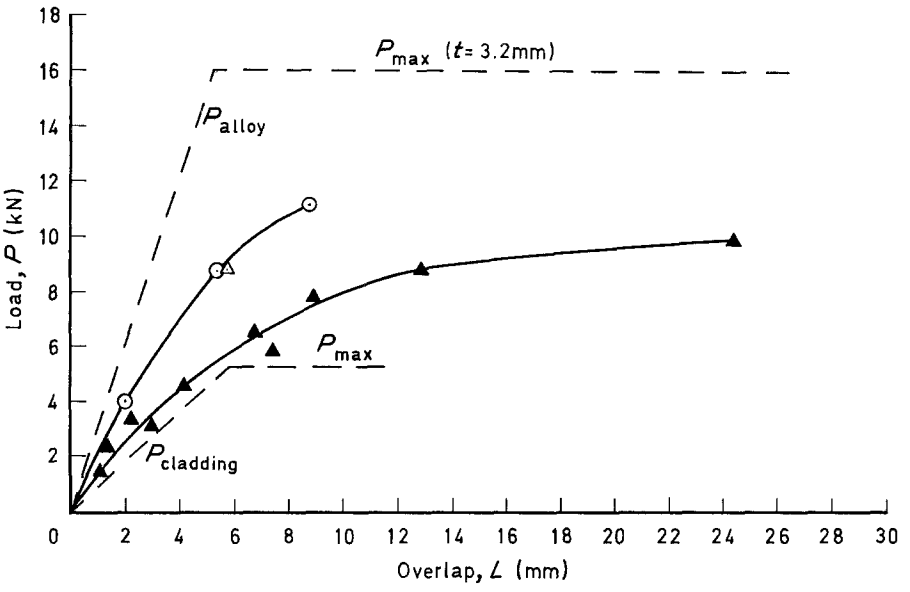

Figure 24 Comparison of failure loads for restrained and unrestrained test pieces, with values calculated for cladding and parent alloys. SHT. Bonding conditions: (○) 280° C, 120 MPa, restrained; (△) 450° C, 7 MPa, restrained; (▲) 450° C, 7 MPa, unrestrained.

References

1. ASME, "Advanced Aluminium and Titanium Structures" (American Society of Mechanical Engineers, Washington, 1981) p. 33.
2. D. V. DUNFORD and P. G. PARTRIDGE, Proceedings of the International Conference, "Superplasticity in Aerospace-Aluminium", Cranfield, July (1985) p. 257.
3. T. D. S. RYAN and R. B. VASTAVA, Proceedings of the Symposium, "Welding, Bonding and Fastening", NASA Pub. 2387, October (1984) p. 231.
4. R. HOLBEIN and K. F. SAHM, Proceedings 2nd International Conference on "Welding and Brazing in Aircraft and Spacecraft Construction", Essen Deutcher Verband Schweisstechnik, No. 98, September (1985) p. 59.
5. I. M. BARTA, *Welding Res. Suppl.* (1964) 241s.
6. G. E. METZGER, "Fabrication of Composite Materials Source Book" (ASM, 1985) p. 171.
7. D. B. ARNOLD, "Developments in Adhesives", Vol 2 (Applied Science, London, 1981) p. 207.
8. A. J. KINLOCH, *J. Mater. Sci.* **17** (1982) 617.
9. E. LUGSCHEIDER, H. REIMANN and O. KNOTEK, *Welding Res. Suppl.* (1977) 189s.
10. L. J. HART-SMITH, "Delamination and Debonding of Materials", ASTM STP 876 (American Society for Testing and Materials, Philadelphia, Pennsylvania, 1985) p. 238.
11. L. J. HART-SMITH, 19th National SAMPE Symposium (1974) p. 722.
12. *Idem*, "Developments in Adhesives", Vol 2 (Applied Science, London, 1981) p. 1.
13. E. M. BREINAN and K. F. KREIDER, *Metals Eng. Q.* **9** (1969) 5.
14. J. HARVEY, P. G. PARTRIDGE and C. L. SNOOKE, *J. Mater. Sci.* **20** (1985) 1009.
15. J. HARVEY, P. G. PARTRIDGE and A. LURSHAY, *Mater. Sci. Eng.* **79** (1986) 191.
16. R. J. SCHWENSFEIR, G. TRENKLER, R. G. DELAGI and J. A. FORSTER, Proceedings of the Symposium, "Welding, Bonding and Fastening", (NASA publication 2387, October 1984) p. 323.
17. P. G. PARTRIDGE, J. HARVEY and D. V. DUNFORD, "Advanced Joining of Metallic Materials", AGARD Conference, Oberammergau, September (1985) Proceedings No 398, July 1986 p. 8-1.
18. N. BREDZS and F. M. MILLER, *Welding Res. Suppl.* (1968) 481.
19. R. L. PEASLEE, *Welding J.* Vol. 55, no. 10 (1976) 850.
20. W. J. TOMLINSON and N. J. BRYAN, *J. Mater. Sci.* **21** (1986) 103.

Received 28 April
and accepted 10 July 1986